472 Inorg. Chem. 2001, 40, 472−477

Connecting Pairs of Dimetal Units To Form Molecular Loops

F. Albert Cotton,[*,†] Chun Lin,[†] and Carlos A. Murillo[*,†,‡]

Department of Chemistry and Laboratory for Molecular Structure and Bonding, P.O. Box 30012,
Texas, A&M University, College Station, Texas 77842-3012, and Department of Chemistry,
University of Costa Rica, Ciudad Universitaria, Costa Rica

Received September 7, 2000

Four compounds consisting of molecular loops formed from two quadruply bonded $Mo_2(DAniF)_2$ (DAniF = *N,N′*-di-*p*-anisylformamidinate) units linked by two dicarboxylate anions have been prepared in high purity and essentially quantitative yields. These compounds have been characterized by crystallography and NMR spectroscopy and display electrochemical behavior dependent on the nature of the dicarboxylate anion. However, the electronic communication between the two Mo_2^{4+} units is not strong. As denoted by the dicarboxylate linkers, the compounds are malonate, **1**, 1,4-phenylendiacetate, **2**, homophthalate, **3**, and *trans*-cyclopentane-1,2-dicarboxylate, **4**.

Introduction

There is now wide interest in creating molecular compounds with various geometries such as triangles, squares, and other polygons as well as polyhedra by assembling corner pieces of appropriate geometry with suitable linkers.[1] For example, to create molecular squares *cis*-ML_2 units, M = Pd, Pt and L_2 = two monodentate phosphines or amines or a chelating diphosphine or diamine, are often used as corner pieces. Four of these corner units can be bound together by four linkers, e.g., those with two nitrogen-containing donor groups. Usually such molecules are cationic with very high charges (e.g., +8), and most of them are electrochemically inactive.

To build similar structures while avoiding these characteristics, our approach has been to use dinuclear corner pieces containing metal−metal bound units bridged by a variable number of formamidinate ligands. This not only leads to neutral products, but because these M_2 units generally show rich electrochemical behavior,[2] it allows positive charge to be introduced systematically. The electrochemical studies can also be used to determine the extent of communication between dinuclear units through the linker or linkers.[3]

When the number of bridging formamidinate, ArNC(H)NAr, groups is three, two such dimetal units (**I**) can be linked by one dicarboxylate group to give compounds in which communication between the two quadruply bonded units can be monitored electrochemically as a function of the linker.[4] For dimetal units with only two bridging formamidinate groups in a cisoid relationship, we have shown[5] that neutral molecular squares and triangles consisting of the dimetal units Mo_2^{4+} and Rh_2^{4+} at the corners can be made. Assemblage of these units is accomplished after substitution of the L ligands in compounds of the type **II** with dicarboxylate anions that have oppositely directed carboxyl groups, **III**. With most such linkers the formation of squares is highly favored by the preferred 90° angle subtended at the dimetal unit, although triangles are sometimes formed.[5,6] However, a different result can be induced by the

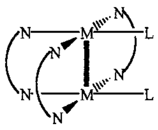

I

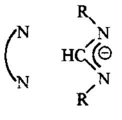

L = CH_3CN

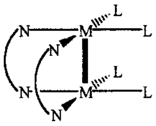

II

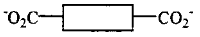

III

IV

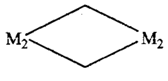

V

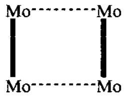

VI

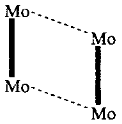

VII

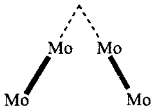

VIII

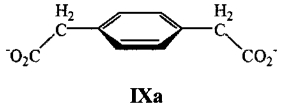

IXa

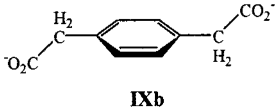

IXb

---

[*] To whom correspondence should be addressed. E-mail: cotton@tamu.edu or murillo@tamu.edu.

[†] Texas A&M University.

[‡] University of Costa Rica.

(1) (a) Leininger, S.; Olenyuk, B.; Stang, P. J. *Chem. Rev.* **2000**, *100*, 853 and references therein. (b) Fujita, M. *Chem. Soc. Rev.* **1998**, *27*, 417, and references therein. (c) Espinet, P.; Soulantica, K.; Charmant, J. P. H.; Orpen, A. G. *Chem. Commun.* **2000**, 915. (d) Navarro, J. A. R.; Lippert, B. *Coord. Chem. Rev.* **1999**, *185−186*, 653. (e) Whang, D.; Kim, K. *J. Am. Chem. Soc.* **1997**, *119*, 451. (f) Mann, S.; Huttner, G.; Zsolnai, Li; Heinze, K. *Angew. Chem., Int. Ed. Engl.* **1996**, *35*, 2808. (g) Scherer, M.; Caulder, D. L.; Johnson, D. W.; Raymond, K. N. *Angew. Chem., Int. Ed. Engl.* **1999**, *38*, 1588. (h) Lai, S.-W.; Chan, M. C.-W.; Peng, S.-M.; Che, C.-M. *Angew. Chem., Int. Ed. Engl.* **1999**, *38*, 669. (i) Jones, C. J. *Chem. Soc. Rev.* **1998**, *27*, 289. (j) Klausmeyer, K. K.; Wilson, S. R.; Rauchfuss, T. B. *J. Am. Chem. Soc.* **1999**, *121*, 2705. (k) Chui, S. S.-Y.; Lo, S. M.-F.; Charmant, J. P. H.; Orpen, A. G.; Williams, I. D. *Science* **1999**, *283*, 1148.

(2) Lin, C.; Protasiewicz, J. D.; Smith, E. T.; Ren, T. *Inorg. Chem.* **1996**, *35*, 6422.

(3) Creutz, C. *Prog. Inorg. Chem.* **1983**, *30*, 1.

(4) Cotton, F. A.; Donahue, J. P.; Lin, C.; Murillo, C. A. *Inorg. Chem.*, accepted.

(5) (a) Cotton, F. A.; Daniels, L. M.; Lin, C.; Murillo, C. A. *J. Am. Chem. Soc.* **1999**, *121*, 4538. (b) Cotton, F. A.; Lin, C.; Murillo, C. A. *Inorg. Chem.* **2001**, *40*, 478.

(6) Cotton, F. A.; Lin, C.; Murillo, C. A. *Inorg. Chem.* **2001**, *40*, 575.

10.1021/ic0010151 CCC: $20.00

Table 1. Crystal and Structure Refinement Data for Compounds **1**−**4**

	1·$2CH_2Cl_2$	**2**·$3.5CH_3CN$	**3**·$2CH_2Cl_2$·$0.5C_8H_{10}$	**4**·$2CH_2Cl_2$
chemical formula	$C_{68}H_{68}Cl_4Mo_4N_8O_{16}$	$C_{87}H_{86.5}Mo_4N_{11.5}O_{16}$	$C_{84}H_{81}Cl_4Mo_4N_8O_{16}$	$C_{76}H_{80}Cl_4Mo_4N_8O_{16}$
fw	1778.86	1932.94	1984.13	1887.04
cryst syst	triclinic	triclinic	triclinic	triclinic
space group	$P\bar{1}$	$P\bar{1}$	$P\bar{1}$	$P\bar{1}$
a, Å	10.670(2)	16.194(3)	11.749(1)	10.182(1)
b, Å	12.529(3)	17.347(3)	16.921(1)	12.959(3)
c, Å	15.588(6)	17.559(3)	22.710(1)	16.153(3)
α, deg	102.30(2)	98.72(1)	103.111(1)	107.54(1)
β, deg	103.43(1)	96.98(1)	95.158(1)	93.38(1)
γ, deg	111.07(2)	114.92(1)	104.508(1)	99.90(1)
V, Å^3	1787.6(9)	4326(1)	4205.1(6)	1988.0(6)
Z	1	2	2	1
temp, K	213(2)	213(2)	213(2)	293(2)
λ, Å	0.710 73	0.710 73	0.710 73	0.710 73
ρ_{calcd}, g cm^{-3}	1.652	1.484	1.567	1.576
μ, mm^{-1}	0.907	0.638	0.780	0.821
R1,[a] wR2[b] $[I > 2\sigma(I)]$	0.071, 0.148	0.070, 0.152	0.046, 0.112	0.085, 0.234
R1, wR2	0.086, 0.164	0.095, 0.169	0.070, 0.129	0.101, 0.253

[a] $R1 = [\sum w(F_o - F_c)^2/\sum wF_o^2]^{1/2}$. [b] $wR2 = [\sum[w(F_o^2 - F_c^2)^2]/\sum w(F_o^2)^2]^{1/2}$, $w = 1/[\sigma^2(F_o^2) + (aP)^2 + bP]$, where $P = [\max(F_o^2,0) + 2(F_c^2)]/3$.

employment of bent dicarboxylate linkers **IV**, whereby *loops* (**V**) are produced. We report here the first family of four neutral dimolybdenum loops composed of two *cis*-Mo2(DAniF)$_2{}^{2+}$ units, DAniF = *N*,*N′*-di-*p*-anisylformamidinate, linked by two dicarboxylate dianions; only one other structure of a compound containing two dimetal units linked by bent dicarboxylate anions has been reported previously, namely, the ionic compound $\{Mo_4[\eta^2,\mu\text{-}O_2C(CH_2)_2CO_2\text{-}\mu,\eta^2]_2(MeCN)_{12}\}(BF_4)_4$.[7]

Experimental Section

General. All the syntheses were performed under a dry nitrogen atmosphere using standard Schlenk techniques. Solvents were dried and then distilled under nitrogen following conventional methods. Chemicals were purchased from Aldrich and used as received. The tetrabutylammonium salts of the dicarboxylic acids were prepared by neutralizing the corresponding acid with 1.0 M $Bu^n{}_4NOH$ in MeOH solution, followed by vacuum-drying at 40−50 °C for 24 h. The compound [*cis*-$Mo_2(DAniF)_2(CH_3CN)_4](BF_4)_2$ was prepared by following published procedures.[8] Elemental analyses were performed by Canadian Microanalytical Service, Delta, British Columbia; the results were satisfactory. The cyclic voltammograms were recorded on a BAS 100 electrochemical analyzer in 0.10 M $Bu^n{}_4NPF_6$ solution (CH_2Cl_2), with Pt working and auxiliary electrodes, a Ag/AgCl reference electrode, and scan rates of 100 mV s^{-1}. All the potential values are referenced to the Ag/AgCl electrode, and under the present experimental conditions, the $E_{1/2}(Fc^+/Fc)$ was consistently measured to be 440 mV.

Preparation of Complexes. [*cis*-$Mo_2(DAniF)_2]_2(O_2CCH_2CO_2)_2$ (1). To a stirred solution of [*cis*-$Mo_2(DAniF)_2(CH_3CN)_4](BF_4)_2$ (104 mg, 0.100 mmol) in 20 mL of CH_3CN was added $(Bu^n{}_4N)_2(O_2CCH_2CO_2)$ (65.0 mg, 0.110 mmol) in 10 mL of CH_3CN. An immediate reaction took place with formation of a bright-yellow precipitate, which was collected by filtration, washed several times with CH_3CN, and dried under vacuum. The crude product was extracted with CH_2Cl_2 (3 × 4 mL). Hexanes were then carefully layered on the top of the solution to afford a yellow crystalline material after several days. Anal. Calcd (found) for **1**, $C_{66}H_{64}Mo_4N_8O_{16}$: C, 49.26 (48.82); H, 4.01 (3.99); N, 6.97 (6.94). ^1H NMR δ (ppm, in CD_2Cl_2): 8.57 (s, 4H, $-NCHN-$), 6.60 (dd, 32H, aromatic), 4.53 (s, 4H, $-O_2CCH_2CO_2-$), 3.69 (s, 24H, $-OCH_3$). A similar method was used for compounds **2**−**4**. Yields were essentially quantitative.

[*cis*-$Mo_2(DAniF)_2]_2(O_2CCH_2C_6H_4CH_2CO_2)_2$ (2). Yellow single crystals suitable for X-ray analysis were grown by diffusion of hexanes into a CH_2Cl_2 solution. Anal. Calcd (found) for **2**, $C_{80}H_{76}Mo_4N_8O_{16}$: C, 53.70 (54.22); H, 4.28 (4.29); N, 6.26 (6.28). ^1H NMR δ (ppm, in CD_2Cl_2): 8.49 (s, 4H, $-NCHN-$), 7.30 (s, 8H, $-CH_2C_6H_4CH_2-$), 6.60 (dd, 32H, aromatic), 4.21 (s, 8H, $-CH_2C_6H_4CH_2-$), 3.69 (s, 24H, $-OCH_3$).

[*cis*-$Mo_2(DAniF)_2]_2$(*o*-$O_2CC_6H_4CH_2CO_2)_2$ (3). Yellow single crystals suitable for X-ray analysis were grown by diffusion of *p*-xylene into a CH_2Cl_2 solution. Anal. Calcd (found) for **3**, $C_{78}H_{72}Mo_4N_8O_{16}$: C, 53.19 (53.57); H, 4.12 (4.15); N, 6.36 (6.30). ^1H NMR δ (ppm, in CD_2Cl_2): 8.52 (s, 2H, $-NCHN-$), 8.50 (d, 2H, $-C_6H_4CH_2-$), 8.35 (s, 2H, $-NCHN-$), 7.44 (m, 6H, $-C_6H_4CH_2-$), 6.65 (m, 32H, aromatic), 3.70 (s, 4H, $-C_6H_4CH_2-$), 3.69 (s, 24H, $-OCH_3$).

[*cis*-$Mo_2(DAniF)_2]_2(O_2CC_5H_8CO_2)_2$ (4). Yellow single crystals suitable for X-ray analysis were grown by diffusion of hexanes into a CH_2Cl_2 solution. Anal. Calcd (found) for **4**, $C_{74}H_{76}Mo_4N_8O_{16}$: C, 51.76 (51.39); H, 4.46 (4.45); N, 6.53 (6.49). ^1H NMR δ (ppm, in CD_2Cl_2): 8.44 (s, 2H, $-NCHN-$), 8.43 (s, 2H, $-NCHN-$), 6.10 (m, 32H, aromatic), 3.80 (br, 4H, $-C_5H_8-$), 3.71 (s, 6H, $-OCH_3$), 3.70 (s, 6H, $-OCH_3$), 3.69 (s, 6H, $-OCH_3$), 3.68 (s, 6H, $-OCH_3$), 2.41 (br, 4H, $-C_5H_8-$), 1.95 (br, 8H, $-C_5H_8-$).

Crystallographic Procedures. Single-crystal X-ray work on compounds **1**, **2**, and **4** was performed on a Nonius FAST diffractometer utilizing the program MADNES.[9] In each case a suitable crystal was mounted on the tip of a quartz fiber with a small amount of silicone grease or epoxy and transferred to a goniometer head. Cell parameters were obtained from an autoindexing routine and were refined with 250 reflections within a 2 Å range of 18.1−41.6°. Cell dimensions and Laue symmetry for all crystals were confirmed with axial photographs. All data were corrected for Lorentz and polarization effects. Data were processed using an ellipsoid-mask algorithm (program PROCOR[10]), and the program SORTAV[11] was used to correct for absorption.

The data for **3** were collected on a Bruker SMART 2000 CCD detector system. Cell parameters were measured using the SMART[12] software. Data were corrected for Lorentz and polarization effects using the program SAINT.[13] Absorption corrections were applied using SADABS.[14] All other data collection procedures were similar to those used on the FAST diffractometer (vide supra).

---

(7) Whelan, E.; Deveraux, M.; McCann, M.; McKee, V. *Chem. Commun.* **1997**, 427.

(8) Chisholm, M. H.; Cotton, F. A.; Daniels, L. M.; Folting, K.; Huffman, J.; Iyer, S.; Lin, C.; Macintosh, A. M.; Murillo, C. A. *J. Chem. Soc., Dalton Trans.* **1999**, 1387.

(9) Pflugrath, J.; Messerschmitt, A. MADNES, Munich Area Detector (New EEC) System, version EEC 11/1/89, with enhancements by Nonius Corporation, Delft, The Netherlands. A description of MADNES appears in the following. Messerschmitt, A.; Pflugrath, J. *J. Appl. Crystallogr.* **1987**, *20*, 306.

(10) (a) Kabsch, W. *J. Appl. Crystallogr.* **1988**, *21*, 67. (b) Kabsch, W. *J. Appl. Crystallogr.* **1988**, *21*, 916.

(11) Blessing, R. H. *Acta Crystallogr.* **1995**, *A51*, 33.

(12) *SMART, Software for the CCD Detector System*, version 5.5; Bruker Analytical Instruments Division: Madison, WI, 1998.

(13) *SAINT, Software for the CCD Detector System*, version 5.06; Bruker Analytical Instruments Division: Madison, WI, 1997.

(14) SADABS. Program for absorption correction using the Bruker CCD based on the Blessing's method (see ref 9).

Table 2. Selected Bond Distances (Å) for Compounds **1**−**4**

	Compound **1**		
Mo(1)−Mo(2)	2.088(1)	Mo(2)−N(4)	2.098(8)
Mo(1)−N(1)	2.117(8)	Mo(2)−N(2)	2.100(8)
Mo(1)−N(3)	2.124(7)	Mo(2)−O(6)	2.130(6)
Mo(1)−O(7)	2.131(6)	Mo(2)−O(8)	2.144(6)
Mo(1)−O(5)	2.136(6)		
	Compound **2**		
Mo(1)−Mo(2)	2.086(1)	Mo(3)−Mo(4)	2.094(1)
Mo(1)−O(9)	2.121(6)	Mo(3)−N(7)	2.107(7)
Mo(1)−N(1)	2.124(7)	Mo(3)−N(5)	2.111(7)
Mo(1)−O(13)	2.131(6)	Mo(3)−O(11)	2.119(6)
Mo(1)−N(3)	2.135(7)	Mo(3)−O(15)	2.128(6)
Mo(2)−N(2)	2.125(7)	Mo(4)−N(8)	2.112(7)
Mo(2)−O(14)	2.139(5)	Mo(4)−N(6)	2.127(7)
Mo(2)−O(10)	2.143(6)	Mo(4)−O(12)	2.138(6)
Mo(2)−N(4)	2.152(7)	Mo(4)−O(16)	2.173(6)
	Compound **3**		
Mo(1)−Mo(2)	2.0879(5)	Mo(3)−Mo(4)	2.0922(4)
Mo(1)−N(1)	2.118(3)	Mo(3)−O(205)	2.102(2)
Mo(1)−N(3)	2.129(3)	Mo(3)−N(5)	2.103(3)
Mo(1)−O(201)	2.133(3)	Mo(3)−O(207)	2.123(3)
Mo(1)−O(203)	2.136(2)	Mo(3)−N(7)	2.126(3)
Mo(2)−N(4)	2.115(3)	Mo(4)−N(8)	2.108(3)
Mo(2)−O(204)	2.131(2)	Mo(4)−N(6)	2.134(3)
Mo(2)−N(2)	2.138(3)	Mo(4)−O(208)	2.138(3)
Mo(2)−O(202)	2.148(2)	Mo(4)−O(206)	2.161(2)
	Compound **4**		
Mo(1)−Mo(2)	2.088(1)	Mo(2)−N(4)	2.107(9)
Mo(1)−N(1)	2.115(9)	Mo(2)−N(2)	2.11(1)
Mo(1)−N(3)	2.143(9)	Mo(2)−O(12)	2.153(7)
Mo(1)−O(11)	2.140(8)	Mo(2)−O(14)	2.134(7)
Mo(1)−O(13)	2.155(7)		

In all structures, the positions of some or all of the non-hydrogen atoms were found via direct methods by way of the program package SHELXTL.[15] For all structures, subsequent cycles of least-squares refinement followed by difference Fourier syntheses revealed the positions of the remaining non-hydrogen atoms. All hydrogen atoms were used in calculated positions. Other details of data collection and refinement for all complexes are given in Table 1. Selected atomic distances are provided in Table 2. Other crystallographic data are available as Supporting Information.

Results and Discussion

Syntheses. Complexes **1**−**4** were prepared by treating [*cis*-$Mo_2(DAniF)_2(CH_3CN)_4](BF_4)_2$ with the corresponding dicarboxylate salt according to the reaction

$$2[\textit{cis}\text{-}Mo_2(DAniF)_2(CH_3CN)_4](BF_4)_2 + 2(NBu^n{}_4)_2(O_2C{-}\square{-}CO_2) \xrightarrow{CH_3CN} [\textit{cis}\text{-}Mo_2(DANiF)_2]_2[O_2C{-}\square{-}CO_2]_2 + 4(NBu^n{}_4)(BF_4) \quad (1)$$

Here $[O_2C{-}\square{-}CO_2]^{2-}$ represents the dianion of malonic acid (methanedicarboxylic acid, $CH_2(CO_2H)_2$), 1,4-phenylenediacetic acid ($C_6H_4(CH_2CO_2H)_2$), homophthalic acid (α-carboxy-*o*-toluic acid, *o*-$HO_2CCH_2C_6H_4CO_2H$), or *trans*-cyclopentane-1,2-dicarboxylic acid ($HO_2CC_5H_8CO_2H$). These anions give rise to compounds **1**, **2**, **3**, and **4**, respectively. The procedures employed in this study are similar to those in the preparation of an $[Mo_2]_3$ triangle,[6] $[Mo_2]_4$ squares,[5] and a $[Mo_2]_6$ cage.[16] It is noteworthy that while yields of **1**−**4** are essentially quantitative, all attempts to isolate crystals from a reaction with the dianion of maleic acid (*cis*-1,2-ethylenedicarboxylic acid) have failed.

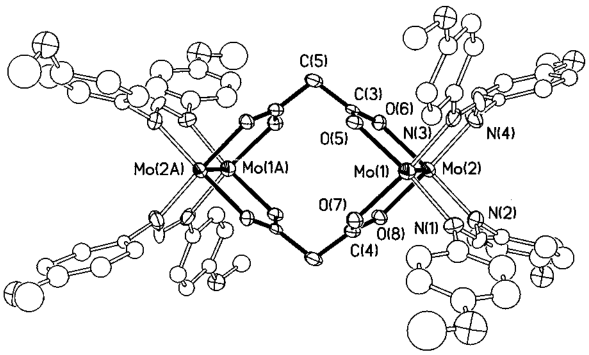

Figure 1. Molecular structure of the malonate loop [*cis*-$Mo_2(DAniF)_2]_2$-$(O_2CCH_2CO_2)_2$ in **1**·$2CH_2Cl_2$ with displacement ellipsoids drawn at the 40% probability level. All hydrogen atoms have been omitted for clarity.

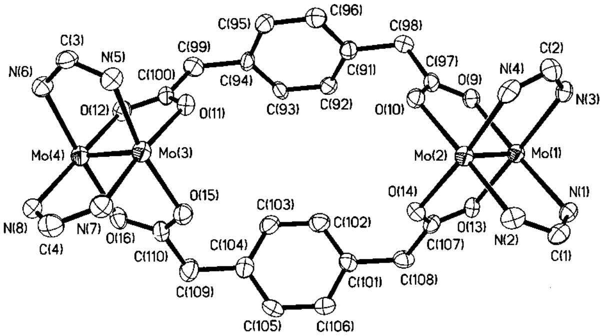

Figure 2. Molecular core structure of the phenylendicarboxylate loop [*cis*-$Mo_2(DAniF)_2]_2(O_2CCH_2C_6H_4CH_2CO_2)_2$ in **2**·$3.5CH_3CN$ with displacement ellipsoids drawn at the 40% probability level.

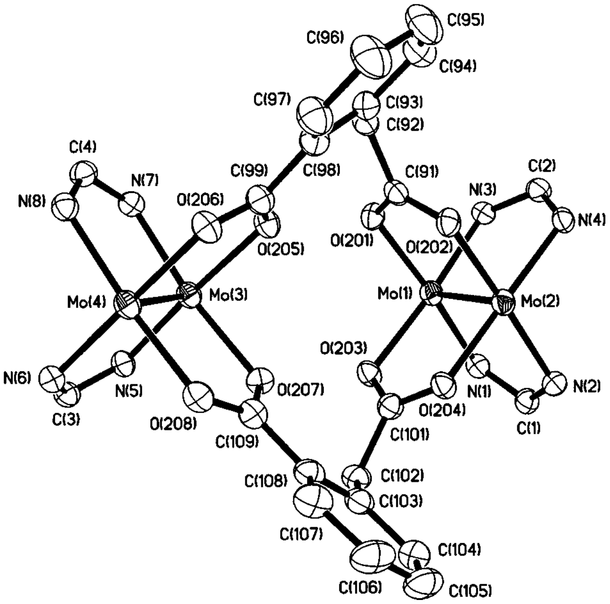

Figure 3. Molecular core structure of the homophthalate loop [*cis*-$Mo_2(DAniF)_2]_2(o\text{-}O_2CC_6H_4CH_2CO_2)_2$ in **3**·$2CH_2Cl_2$·$0.5C_8H_{10}$ with displacement ellipsoids drawn at the 40% probability level.

Structural Results. The X-ray structures of compounds **1**−**4** are depicted in Figures 1−4, respectively. The four compounds crystallize in the triclinic space group $P\bar{1}$, with $Z = 1$ for compounds **1** and **4** and $Z = 2$ for **2** and **3**. About each dimolybdenum unit there is an eclipsed paddlewheel conformation consisting of two cis formamidinate paddles and two carboxylate groups. The entire assembly can be described as a molecular loop. There is a crystallographic inversion center in

---

(15) *SHELXTL*, version 5.03; Siemens Industrial Automation, Inc.: Madison, WI.

(16) Cotton, F. A.; Daniels, L. M.; Lin, C.; Murillo, C. A. *Chem. Commun.* **1999**, 841.

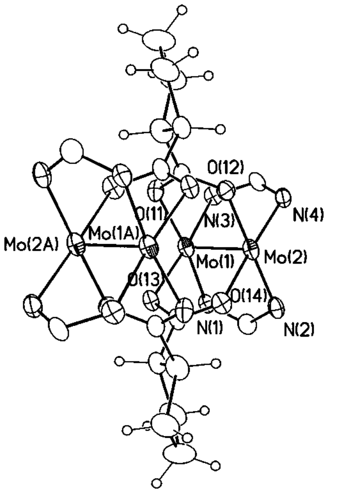

Figure 4. Molecular core structure of the pentanedicarboxylate loop $[cis\text{-}Mo_2(DAniF)_2]_2(O_2CC_5H_8CO_2)_2$ in $\mathbf{4}\cdot 2CH_2Cl_2$ with displacement ellipsoids drawn at the 40% probability level.

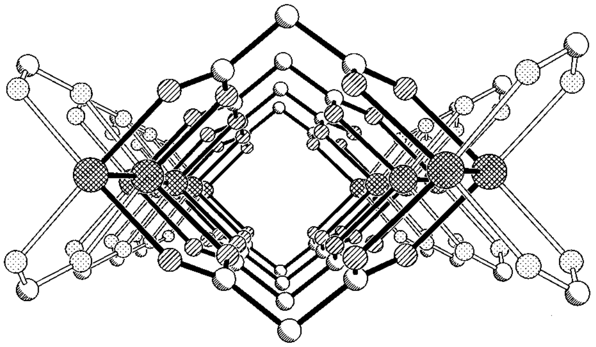

Figure 5. Simplified diagram of **1** showing the channel created by the stacking of molecules in the crystal. The *p*-anisyl groups attached to each nitrogen atom, the hydrogen atoms, and the interstitial solvent molecules have been omitted for clarity.

1 and **4**, while there is an idealized mirror plane defined by all four Mo atoms in compounds **2** and **3**. The crystallographically independent Mo−Mo distances are 2.088(1) Å for **1**, 2.086(1), 2.094(1) Å for **2**, 2.0879(5), 2.0922(4) Å for **3**, and 2.088(1) Å for **4**; these are typical quadruply bonded Mo_2 distances. Other bond distances and bond angles for all compounds are similar to those found in other dimolybdenum paddlewheel complexes and require no further comment. However, it is relevant to discuss the differences in how the vectors along the Mo−Mo bond are oriented. For **1** and **4** the two vectors along the two dimetal units are essentially parallel, but for **1** they adopt the rectangular structure **VI**, while for **4** a rhomboid, **VII**, forms. Thus, the idealized symmetry of **1** is D_{2d}, while it is C_s for **4**. For **2** and **3**, the two vectors converge as in **VIII** with angles of 103° and 64° for **2** and **3**, respectively.

For compound **1**, where the linker is the malonate dianion, the formation of a loop is practically unavoidable in view of the inherently bent nature of this anion. There is no reasonable conformation that can cause the carboxyl groups to be oppositely directed, as would be required to form a square. However, for the 1,4-phenylenediacetic acid, the bent conformation is not a requirement, as shown in **IX**. The conformation **IXb** could have been employed to form a molecular square. Whether or not the latter can also be made is still uncertain. So far we have not been able to observe it.

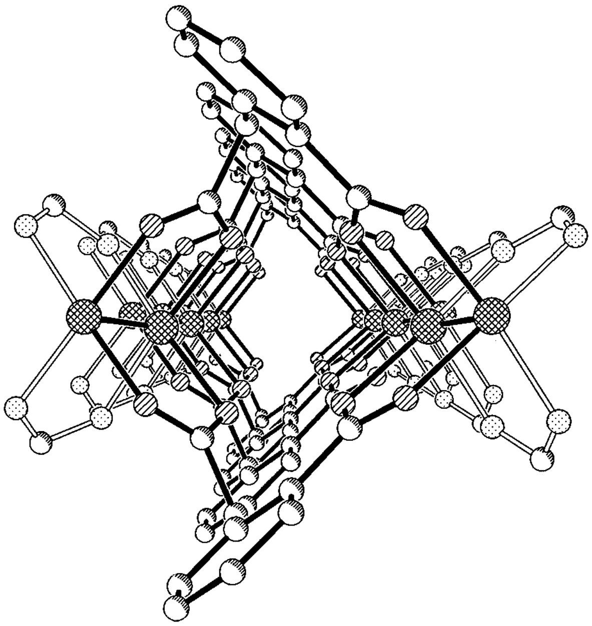

Figure 6. Simplified diagram of **3** showing the channel created by the stacking of molecules in the crystal. The *p*-anisyl groups attached to each nitrogen atom, the hydrogen atoms, and the interstitial solvent molecules have been omitted for clarity.

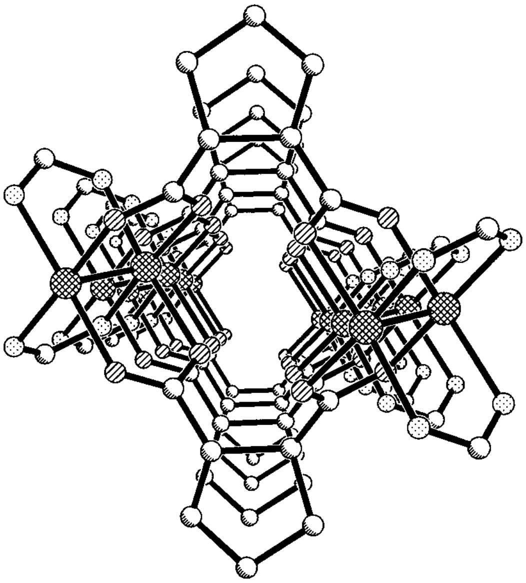

Figure 7. Simplified diagram of **4** showing the channel created by the stacking of molecules in the crystal. The *p*-anisyl groups attached to each nitrogen atom, the hydrogen atoms, and the interstitial solvent molecules have been omitted for clarity.

The crystal packing patterns of these compounds are also interesting. In **1**, **3**, and **4**, molecular loops stack directly on top of each other, creating a channel, as shown in Figures 5, 6, and 7, respectively. Similar packing patterns were also found in some $[Mo_2]_4$, $[Rh_2]_4$ squares, and the $[Rh_2]_3$ triangle.[5] Compound **2** adopts a different packing pattern in which alternating layers of loops are offset, as shown in Figure 8. Therefore, channels are not formed.

Solution Behavior. ^1H NMR spectra show that all compounds are prepared in high purity, but there are interesting differences that can be associated with the corresponding structures. For **1** there is only one type of DAniF ligand as indicated by the unique methine and methoxy signals. Likewise, the unique methylene signal indicates that all linkers are equivalent in solution. These observations are consistent with the symmetrical solid-state structure.

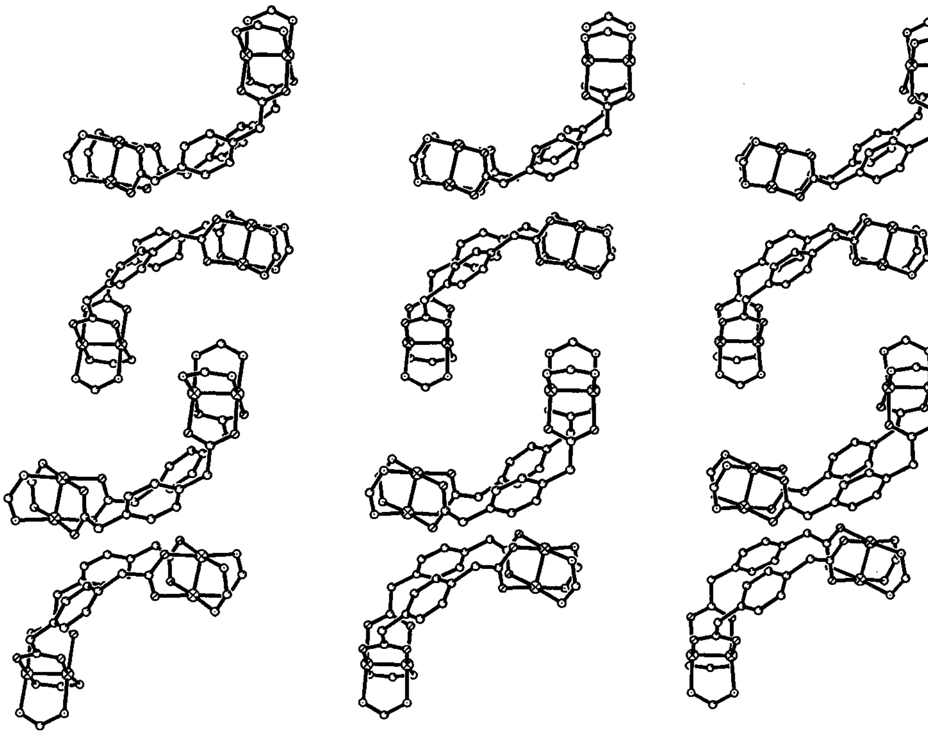

Figure 8. Simplified packing diagram of **2**. Note how the loops are offset, preventing the formation of channels. The *p*-anisyl groups attached to each nitrogen atom, the hydrogen atoms, and the interstitial solvent molecules have been omitted for clarity.

Table 3. Comproportionation Constants Derived from Electrochemical Data[a] for Compounds **1**−**3**[b]

Compd.	Peak Positions in DPV, mV	$\Delta E_{1/2}$ [c]	K_c [d]
1	$\xrightarrow{-e}$ 405 $\xrightarrow{-e}$ 477	109	70
2	$\xrightarrow{-2e}$ 327	91	35
3	$\xrightarrow{-e}$ 169 $\xrightarrow{-e}$ 293	179	$1.1\text{x}10^3$

[a] The electrochemical data were recorded on a BAS 100 electrochemical analyzer in 0.10 M $Bu^n{}_4NPF_6$ solution (CH_2Cl_2) with Pt working and auxiliary electrodes and a Ag/AgCl reference electrode. Scan rate was 100 mV s^{-1} for CV and 4 mV s^{-1} for DPV. All potential values are referenced to the Ag/AgCl, and under the present experimental conditions, the $E_{1/2}(Fc^+/Fc)$ was consistently measured to be 440 mV. [b] A comproportionation constant cannot be calculated for **4** because of the irreversibility of its oxidation wave. [c] $\Delta E_{1/2}$ was calculated by the Richardson and Taube method by measuring the DPV peaks at half-height (see ref 16). [d] The comproportionation constants, K_c, were calculated from the formula $K_c = \exp(\Delta E_{1/2})/25.69$), as in ref 17.

For **2**, the NMR data also show that the methine protons are also equivalent. This is not what would be expected if the solid-state structure remained unchanged. Because of the orientation of the aromatic rings in the linker with respect to the carboxyl groups, one would expect two sets of methine signals. However, similar linkers are known to be flexible. For example, in compounds $[(en)Pd]_2(PyCH_2XCH_2Py)_2$ (en = ethylenediamine, X = none or $-C_6F_4-$), the orientation of the linkers in solution are also symmetrical as indicated by their ^1H NMR spectra.

For both **3** and **4** there is a pair of singlets at 8.52 and 8.35, and 8.44 and 8.43 ppm, respectively. Each singlet corresponds to two methine hydrogen atoms. This indicates that the less symmetrical solid-state structure persists in solution. Evidently these dicarboxylate linkers are less flexible. Interestingly, all CH_3 hydrogen atoms of the *p*-anisyl groups give one degenerate signal for **3**, but there are four very closely spaced signals of equal intensity for **4**.

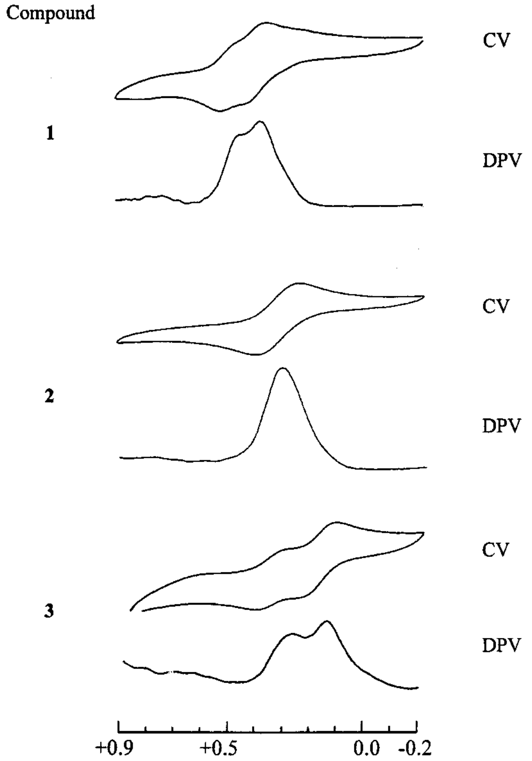

Figure 9. Cyclic voltammograms (CV) and differential pulse voltammograms (DPV) of compounds **1**−**3**.

Electrochemistry. Compounds **1**−**4** have been examined carefully by both cyclic voltammetry and differential pulse voltammetry; the results are listed in Table 3 and displayed in Figure 9. Clearly, the electrochemical behavior of this family of neutral compounds is rich, which is in contrast to the report that the ionic compound $\{Mo_4[\eta^2,\mu\text{-}O_2C(CH_2)_2CO_2\text{-}\mu,\eta^2]_2(MeCN)_{12}\}(BF_4)_4$ is not electroactive.[2] It is not obvious why there is such a marked difference.

In **1**, there are two partly resolved one-electron oxidation peaks separated by about 72 mV. In compound **2**, instead of separate peaks there is only one at a potential of 327 mV. However, in compound **3**, there are again two peaks separated by 124 mV. However, in compound **4**, there is only one irreversible peak at E_{pa} of 505 mV. The data for **1**−**3** can be interpreted using the method of Richardson and Taube, which correlates the $\Delta E_{1/2}$ with the width at half-height of the differential pulse voltammogram (DPV) peaks. In this way the values of 109, 91, and 179 mV are obtained for the $\Delta E_{1/2}$ of **1**, **2**, and **3**, respectively. From these $\Delta E_{1/2}$ values the equilibrium constants for comproportionation,

$$[\mathrm{Mo_2}](\mathrm{O_2CXCO_2})_n[\mathrm{Mo_2}] + [\mathrm{Mo_2}^+](\mathrm{O_2CXCO_2})_n[\mathrm{Mo_2}^+] = 2\{[\mathrm{Mo_2}](\mathrm{O_2CXCO_2})_n[\mathrm{Mo_2}]\}^+ \quad (2)$$

can be calculated by using the equation $K_c = \exp(\Delta E_{1/2}/25.69)$. All these results are summarized in Table 3. It is evident that while the Mo_2 units are coupled by the bridging dicarboxylate ion, the coupling is not very strong. However, if there were no coupling at all, the comproportionation constant would have the statistical value of 4.

In attempting to understand the variation in the coupling from one compound to another, one might first ask whether it is a simple function of distance between the Mo_2 units. Qualitatively, such a relationship does exist: The $\Delta E_{1/2}$ values decrease in the order **3** $\gg$ **1** $>$ **2**, and the distances 6.272, 6.512, and 9.624 Å increase in the same order, but no quantitative correlation is evident. If we look instead at the number of carbon atoms between the carboxyl groups, there is no correlation because these go in the order 3, 1, 6 for compounds **3**, **1**, and **2**, respectively. Clearly it is the electronic nature of the connecting groups that controls the extent of communication, but in ways that are not evident at present.

The irreversibility of the electrochemical oxidation of **4** indicates that upon oxidation there is a major change in the structure. This is quite rare for compounds of the types [*cis*-$Mo_2(DAniF)_2(O_2C{-}X{-}CO_2)]_n$. So far only a molecular triangle[6] where $n = 3$ and the linker is the *trans*-cyclohexanedicarboxylate dianion show a similar behavior. A comparison of **3** and **4** shows that while the two compounds are structurally similar, the electrochemical behavior is quite different. In **4** the linker has a nonaromatic five-membered ring, while in **3** there is an aromatic six-membered ring. It is likely that this plays an important role in the stabilization of the oxidized species.

Another interesting but puzzling comparison can be made between compound **1** and the previously reported $(DAniF)_3Mo_2O_2CCH_2CO_2Mo_2(DAniF)_3$.[4] The comproportionation constants are 70 and 67 for **1** and the latter compound, respectively; these values are equal within experimental error. One might have expected **1** to display significantly greater coupling for two reasons. (1) In **1** there are two malonate connectors rather than one, and (2) the distance between the Mo_2 centers is 1.4 Å shorter in compound **1** than it is in the singly bridged compound. It is surprising, to say the least, that neither of these factors appears to matter.

Acknowledgment. We are grateful to the National Science Foundation for support of this work.

Supporting Information Available: An X-ray crystallographic file, in CIF format. This material is available free of charge via the Internet at http://pubs.acs.org.

IC0010151